Numerical simulation of the thermal response of continuous-wave terahertz irradiated skin*

XU De-gang(徐德刚)**, **LIU Chang-ming**(刘长明), **WANG Yu-ye**(王与烨), **WANG Wei-peng**(王卫鹏), **JIANG Hao**(蒋浩), **ZHANG Zhuo**(张卓), **LIU Peng-xiang**(刘鹏翔), **and YAO Jian-quan**(姚建铨)

Key Laboratory of Optoelectronic Information Technology Science, Ministry of Education of China, Institute of Laser and Optoelectronics, College of Precision Instruments and Optoelectronic Engineering, Tianjin University, Tianjin 300072, China

(Received 9 August 2012)
©Tianjin University of Technology and Springer-Verlag Berlin Heidelberg 2013

We report a two-layer model to describe the thermal response of continuous-wave (CW) terahertz (THz) irradiated skin. Based on the Pennes bio-heat conduction equation, the finite element method (FEM) is utilized to calculate the temperature distribution. The THz wave with a Gaussian beam profile is used to simulate the photo-thermal mechanism. The simulation results show the dynamic process of temperature increasing with irradiation time and possible thermal damage. The factors which can affect temperature distribution, such as beam radius, incident power and THz frequency, are investigated. With a beam radius of 0.5 mm, the highest temperature increase is 3.7 K/mW.

Document code: A **Article ID:** 1673-1905(2013)01-0073-4
DOI 10.1007/s11801-013-2303-4

Terahertz (THz) wave has the advantages of low photon energy, low scattering and high transmitting rate for non-polar materials[1]. Applications of THz wave have widely developed in aspects of imaging in bio-tissues and medicine, drug inspection, security monitor, communication, and water concentration measurement[2-6]. However, exposure to THz radiation may lead to instability in living organisms. In some experiments, people have found some unusual phenomena coming up in THz irradiation, e.g. unconventional behavior of male mice[7], abnormal dynamics of DNA[8] and infringement of neurons cellular membranes[9]. The European THz-bridge project[10] firstly proposed to define the safe exposure standards for pulsed and continuous-wave (CW) THz biomedical applications in 2004. Few international organizations determine the skin damage threshold so far. Danielle R. Dalzell et al[11] used the free electron laser (FEL) to determine the damage threshold of tissue ED_{50} to be 7.16 W/cm^2 in pulsed THz radiation. This value is well agreement with their predicted damage threshold of 5.0 W/cm^2 using a computational model in Ref.[11].

In this paper, based on the classical Pennes bio-heat conduction equation, we utilize a two-layer model to simulate the CW THz thermal effect on skin. The dynamic process of temperature change is calculated. The CW THz source with Gaussian beam profile is used in our model. The simulation results show the temperature distribution and the relationships between the optical parameters (beam radius, power) and the temperature distribution. The optical parameters have very small influence on the time required to reach a steady state.

Skin can be divided into two layers: the epidermis and the dermis. The thicknesses of the epidermis and the dermis are about 0.05−0.15 mm and 3 mm, respectively. We establish a cylindrical two-layer model with radius b in Fig.1. The top layer with thickness d_1 represents the epidermis, and the lower layer with thickness d_2 represents the dermis. The THz beam with radius a irradiates the center of the top surface. It also shows the initial boundary conditions for the temperature of each surface A, B, C, D and E.

The classical Pennes bio-heat conduction equation[12] is used in our simulation, which is the most commonly used model to describe the thermal behavior of bio-tissues

$$\rho c\frac{\partial T}{\partial t}=\nabla\cdot[k(T)\nabla T]+Q_r+Q_{\mathrm{m}}+w_{\mathrm{b}}c_{\mathrm{b}}\rho_{\mathrm{b}}(T_{\mathrm{b}}-T)\ , \qquad (1)$$

where ρ is the density of bio-tissue, c is the specific heat of

* This work has been supported by the National High Technology Research and Development Program of China (863 Program) (No.2011AA010205), the National Natural Science Foundation of China (Nos.61172010 and 61107086), and the Natural Science Foundation of Tianjin in China (No. 11JCYBJC01100).

** E-mail:xudegang@tju.edu.cn

bio-tissue, T is the temperature distribution function with r (the radial distance from axis) and z (distance from the top surface of epidermis), and k is the thermal conductivity of bio-tissue. Q_r is the dissipated power density, and Q_m is the metabolic rate, which is usually neglected because it is trifle compared with laser source. w_b is the blood perfusion rate, c_b is the blood specific heat, r_b is the blood density, and T_b is the temperature of artery.

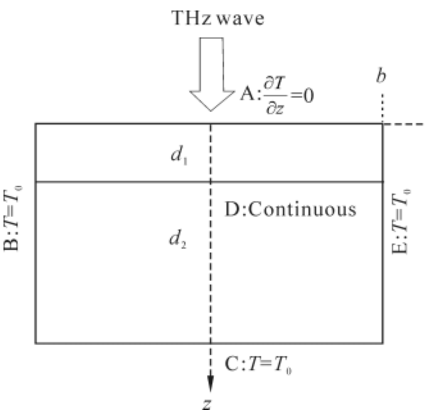

Fig.1 Two-layer model of skin in cylinder coordinates system

We calculate the dissipated power densities of epidermis layer Q_{r_1} and the dermis layer Q_{r_2}. The dissipated power values within epidermis layer Ω_1 and dermis layer Ω_2 are defined to be P_1 and P_2, respectively. P is the total dissipated power. They can be obtained:

$$P=P_1+P_2 \ , \tag{2}$$

$$P_1 = \iiint\limits_{\Omega_1} Q_{r1}\, \mathrm{d}v_1 \ , \tag{3}$$

$$P_2 = \iiint\limits_{\Omega_2} Q_{r2}\, \mathrm{d}v_2 \ . \tag{4}$$

For THz wavelength is longer than that of infrared wave, THz radiation is less susceptible to scattering in bio-tissues[13]. The broadening of beam radius caused by scattering is negligible in this paper. We define α and β as the absorption coefficients of the epidermis layer and dermis layer, respectively. Then there is

$$\frac{P_1}{P_2} = \frac{\int_0^{d_1} \exp(-\alpha z)\,\mathrm{d}z}{\int_{d_1}^{d_1+d_2} \exp(-\beta z)\,\mathrm{d}z} \ . \tag{5}$$

Solving Eqs. (2)-(5), for the Gaussian beam profile, we obtain

$$Q_{r_1}(r,z) = \frac{P_1}{P_1+P_2}\frac{2P\alpha}{\pi a^2}[1-\exp(-\alpha d_1)]^{-1}\exp[-(2r^2/a^2)]\times \exp(-\alpha z), \tag{6}$$

$$Q_{r_2}(r,z) = \frac{P_2}{P_1+P_2}\frac{2P\beta}{\pi a^2}\{\exp(-\beta d_1)-\exp[-\beta(d_1+d_2)]\}^{-1}\times \exp[-(2r^2/a^2)]\cdot\exp(-\beta z) \ . \tag{7}$$

To solve the heat conduction equation, we still need to set the boundary conditions in Fig.1. For the top surface A, it is proper to neglect the loss of heat and set it to be heat isolated. The side surfaces of B, E and bottom surface of C are far from the source, and it is reasonable to set their temperature to be body temperature T_0. The initial boundary D should satisfy the continuous conditions.

The finite element method (FEM) is utilized to calculate the temperature distribution. Values of the absorption coefficients α and β vary for different individuals and tissues. It is a good idea to adopt their mean values. We utilize the linear absorption coefficient values 115 cm^{-1} for α and 85 cm^{-1} for β at 1 THz[14]. The parameters ρ, c and k can be obtained by Eqs.(8)-(10) in Ref.[15]. We neglect the influence of temperature increase on these parameters[16]

$$\rho = (1.3-0.3W) \ \ (\mathrm{g\cdot cm^{-3}}) \ , \tag{8}$$

$$c = (0.37+0.63\frac{W}{\rho}) \ \ (\mathrm{cal\cdot g^{-1}\cdot K^{-1}}) \ , \tag{9}$$

$$k = (0.133+1.36\frac{W}{\rho}) \ \ (\mathrm{cal\cdot cm^{-1}\cdot s^{-1}\cdot K^{-1}}) \ . \tag{10}$$

The water content W is about 50% for the epidermis and 70% for the dermis. The initial values for the simulation are as follows: skin temperature T_0=310.15 K, P=1 mW, a=0.5 mm, d_1=0.1 mm, d_2=3 mm and b=40 mm.

In Fig.2, the temperature curve of t=0 s means the temperature distribution without THz irradiation. As the irradiation time goes on, the heat diffusion causes the temperature rise. The temperature increases fast during the first 30 s. After 150 s, all curves trend to overlap and reach a steady state. The temperature distribution profiles satisfy the exponential attenuation profile along the z direction, since the transmit-

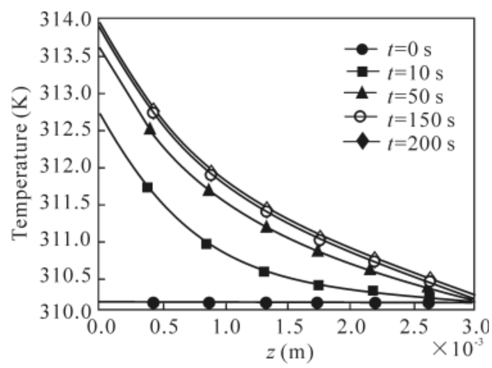

Fig.2 Temperature distributions at *r* =0 along the *z* direction with different irradiation time

ted power decreases exponentially along the z direction. The maximum temperature increase at (r=0, z=0) is 3.7 K.

In Fig.3(a), as the beam radius decreases, the temperature increase becomes larger. It is because the power density is higher for THz source with a small beam radius. In Fig.3 (b), the temperature increase is proportional to the power. The maximum value is 3.7 K/mW approximately. Generally, the values of absorption coefficients increase as the frequency increases[14,17]. For 0.75 THz, 1 THz and 1.25 THz, α is about 90 cm^{-1}, 115 cm^{-1} and 145 cm^{-1}, respectively, and β is about 70 cm^{-1}, 85 cm^{-1} and 100 cm^{-1}, respectively[14]. For higher THz frequency, the temperature is higher in a steady state. In Fig.3, we still can see that the optical parameters have very small influence on the time required to reach a steady state.

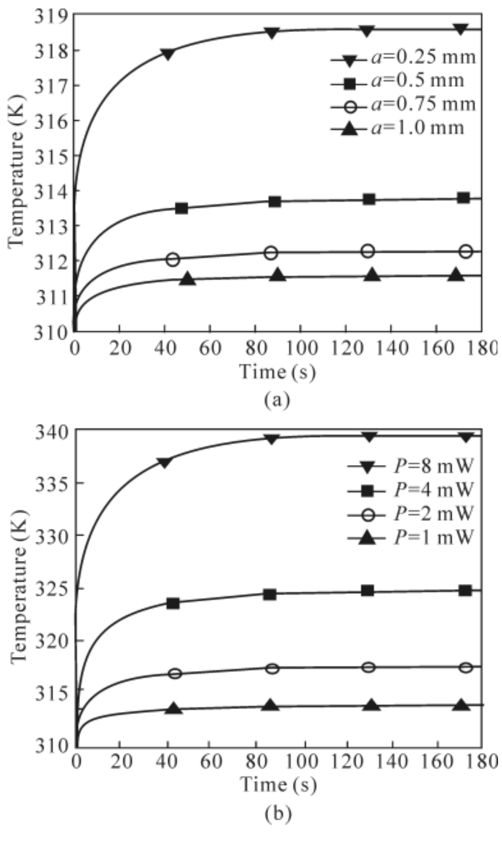

Fig.3 Temperature versus time for THz waves with (a) different beam radii and (b) different power values

In Fig.4, we show the process of temperature (K) rising with irradiation time. The real line in the figures is the initial boundary D. The temperature increases fast during the first 15 s, and becomes constant after about 150 s. The highest temperature is in the center of the air-epidermis surface. The heating up mainly occurs near the top layer, because the absorption coefficients are large for which the typical value is at the order of 10^2 cm^{-1} and the penetration depth of THz beam is restricted. According to Lambert-Beer law,

$$\frac{I}{I_0} = \exp[-\alpha d_1 - \beta(0.5 - d_1)] \approx 0.008 , \tag{11}$$

where I_0 and I are the intensities of the incident beam and the transmitted beam, respectively. So the attenuation of a THz beam penetrating through 0.5 mm in the model is about 1−0.8% = 99.2%.

The conversion of radiant energy to thermal energy can heat the tissue, and induce an injury as the temperature increases. The damage parameter Ω, which indicates the level of damage, is computed using the Arrhenius equation[18]:

$$\Omega(z) = A\int_0^t \exp(-\frac{E}{RT(z,t)})\,\mathrm{d}t \quad , \tag{12}$$

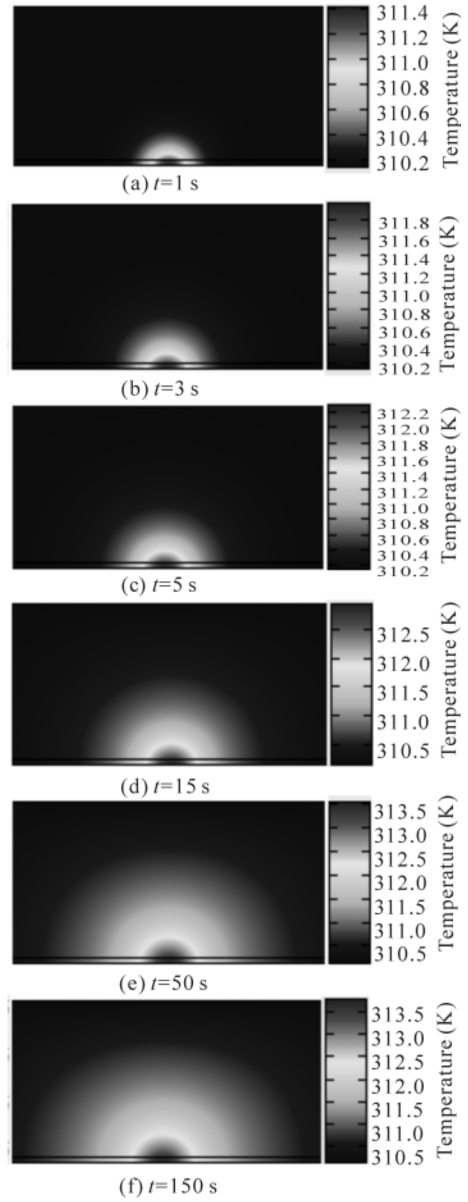

Fig.4 Contours of temperature distribution with different irradiation time

where A is the pre-exponential factor (s^{-1}), E is the activation energy for the reaction (J•mol^{-1}), R=8.31 J•mol^{-1}•K^{-1} is the universal gas constant, and T is the absolute temperature (K). For T between 37 °C and 44 °C, the values A=3.1 × 10^{98} s^{-1} and E=1.5×10^5 J•mol^{-1} are used in calculation. Takata gave the values of A and E for various ranges of tissue temperatures as follows[19]: for T between 44 °C and 50 °C, A=4.3 × 10^{64} s^{-1} and E=4.18 × 10^5 J•mol^{-1}; for T greater than 50 °C, A=9.4 × 10^{104} s^{-1} and E=6.68 × 10^5 J•mol^{-1}.

Henriques and Moritz[18] assigned Ω = 0.53 corresponding to a threshold of the first-degree burn (persistent but reversible erythema), Ω = 1 to the threshold of the second-degree burn (irreversible partial-thickness injury), and Ω = 10000 to a threshold of the third-degree burn (irreversible full-thickness injury). At the same irradiance, the thermal damage of different skin depths is very different, and we compute the possible thermal damage Ω of regional tissue at different time using the Arrhenius equation. The relationships between the thermal damage and skin depth with different irradiation time are described in Fig.5, where the incident power is P=20 mW, radius is r=1 mm, and d is the skin depth.

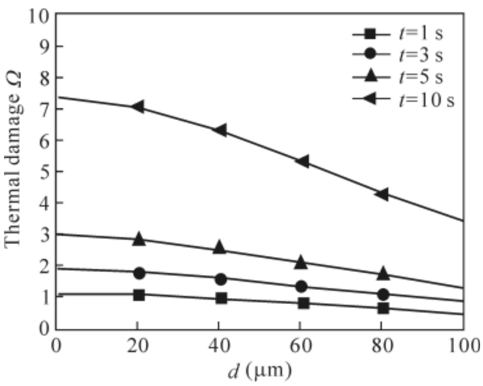

Fig.5 Thermal damage Ω of different epidermis skin depths at t = 1 s, 3 s, 5 s and 10 s, respectively

In summary, from the results of numerical simulation, we study the dynamic process of temperature rising with time, and it takes about 150 s to reach a steady state. The influence of optical parameters on the time required to reach a steady state is limited. Steady temperature calculated with incident power should be higher than actual temperature due to ignoring the reflection on the interface of skin and air. However, as a common simulation, the calculation is ready to change with the parameters and acquires new results of tissues. At last, we compute the thermal damage Ω of different skin depths at different time using the Arrhenius equation. This work may motivate further study on the security of CW THz irradiated bio-tissues.

References

[1] J. F. Federici, B. Schulkin, F. Huang, D. Gary, R. Barat, F. Olivheira and D. Zimdars, Semicondutor Science and Tech nology **20**, S266 (2005).

[2] E. Pickwell, A. J Fitzgerald, P. F. Taday, B. E. Cole, R. J. Pye, T. Ha, M. Pepper and V. P. Wallace, 29th Int. Conf. Infrared, Millimeter, and Terahertz Waves, 821 (2004).

[3] K. Kawase, Y. Ogawa and Y. Watanabe, Optics Express **11**, 2549 (2003).

[4] CHEN Tao, HU Ming, LIANG Ji-ran, HOU Ji-bao, LÜ Zhi-jun and LI Li, Journal of Optoelectronics • Laser **22**, 1348 (2011). (in Chinese)

[5] ZHANG Yu-ping, LIU Ling-yu, ZHANG Xiao, ZHANG Hong-yan and ZHANG Hui-yun, Journal of Optoelectronics • Laser **23**, 832 (2012). (in Chinese)

[6] Y. Y. Wang, H. Minamide, M. Tang, T. Notake and H. Ito, Optics Express **18**, 15504 (2010).

[7] N. P. Bondar, I. L. Kovalenko, D. F. Avgustinovich, A. G. Khamoyan and N. N. Kudryavtseva, Bulletin of Experimental Biology and Medicine **145**, 401 (2008).

[8] B. S. Alexandrov, V. Gelev, A. R. Bishop, A. Usheva and K. Ø. Rasmussen, Physics Letters A **374,** 1214 (2010).

[9] J. S. Olshevskaya, A. S. Ratushnyak, A. K. Petrov, A. S. Kozlov and T. A. Zapara, IEEE Region 8 International Conference on Computational Technologies in Electrical and Electronics Engineering, 210 (2008).

[10] G. P. Gallerano, E. Grosse, R. Korenstein, M. Dressel, W. Mantele, M. R. Scarfi, A. C. Cefalas, P. Taday, R. H. Clothier and P. Jepsen, Joint 29th International Conference on Infrared and Millimeter Waves and 12th International Conference on Terahertz Electronics F7.1, 817 (2004).

[11] D. R. Dalzell, J. McQuade, R. Vincelette, B. Ibey, J. Payne, R. Thomas, W. P. Roach, C. L. Roth and J. Wilmink, Proc. SPIE **7562**, 75620M (2010).

[12] H. H. Pennes, Journal of Applied Physiology **1**, 93 (1948).

[13] P. Y. Han, G. C. Cho and X. C. Zhang, Optics Letters **25**, 242 (2000).

[14] E. Berry, A. J. Fitzgerald, N. N. Zinov'ev, G. C. Walker, S. Homer-Vanniasinkam, C. D. Sudworth, R. E. Miles, J. M. Chamberlain and M. A. Smith, Proc. SPIE **5030**, 459 (2003).

[15] A. J. Welch, IEEE J. Quantum Electron. **20**, 1471 (1984).

[16] V. V. Tuchin, Y. N. Scherbakov, A. N. Yakumin and I. V. Yaroslavsky, SPIE **PM25**, 100 (1995).

[17] V. P. Wallace, A. J. Fitzgerald, E. Pickwell, R. J. Pye, P. F. Taday, N. Flanagan and T. Ha, Applied Spectroscopy **20**, 1127 (2006).

[18] F. C. Henriques and A. R. Moritz, Arch. Pathol. **43**, 489C502 (1947).

[19] A. N. Takata, Aerospace Med. **45**, 634 (1974).